Intercomparison of Integrated Water Vapor Estimative from Multi-sensor in Amazonian Regions

Luiz F. Sapucci[1], Luiz A. T. Machado[1], João F. G. Monico[2], Artemio Plana-Fattori[3,4].

1. Centro de Previsão de Tempo e Estudos Climáticos, Instituto Nacional de Pesquisas Espaciais, Cachoeira Paulista São Paulo, Brazil.

2. Departamento de Cartografia da Faculdade de Ciências e Tecnologia da Universidade Estadual Paulista, Presidente Prudente, São Paulo, Brazil.

3. Departamento de Ciências Atmosféricas - Instituto de Astronomia, Geofísica e Ciências Atmosféricas da Universidade de São Paulo, São Paulo, São Paulo, Brazil.

4. Laboratoire d'Optique Atmosphérique, Université des Sciences et Technologies de Lille, France.

Submitted to Journal of Atmospheric and Oceanic Technology - July 2006.

ABSTRACT

Water vapor is an atmospheric component of major interest in atmospheric science, because it affects the energy budget and plays a key role in the several atmospheric processes. The Amazonian region is one of the most humid on the planet and land use change is able to affect the hydrologic cycle in several areas and consequently to generate severe modifications in the global climate. Within this context, accessing the error associated with atmospheric humidity measurement and the validation of IWV quantification from different techniques is very important in these regions. Using data collected during RACCI/DRY-TO-WET (Radiation, Cloud, and Climate Interactions in Amazonia during the DRY-TO-WET Transition Season) an experiment carried out in Southwestern Amazonia in 2002, this paper presents quality analysis of IWV (Integrated Water Vapor) measurements from RS80 radiosondes, a suite of GPS (Global Positioning System) receivers, an AERONET (AErosol RObotic NETwork) solar radiometer, and humidity sounding from HSB (Humidity Sounder for Brazil) aboard the AQUA satellite. When compared to RS80 IWV values, the RMS (Root Mean Square) from the AERONET and HSB sensor and GPS are to the order of 2.7, 7.7 and 4.3 kg m^{-2}, respectively. The difference generated between IWV from the GPS receiver and RS80 during daytime was larger than the nighttime period due to the combination of the influence of high ionospheric activity during the RACCI experiment and a daytime drier bias from the RS80.

1. Introduction

There is a consensus that atmospheric water vapor plays a crucial role in the atmospheric processes. This atmospheric component makes the largest contribution to the greenhouse effect

and its distribution is associated with cloud concentration and rainfall. Water vapor advection and the release of latent heat influence the vertical stability and the structure and evolution of atmospheric storm systems.

Water vapor is the atmospheric component that has the greatest temporal and spatial variability. It can vary by several orders of magnitude in location and height during a short period of time. Low precision and a lack of continuous water vapor measurement is one of the major error sources for short-term precipitation forecasts (Kuo 1996). Nowadays, to minimize the effect of such error in numerical weather prediction, several devices are used to operationally measure IWV (Integrated Water Vapor), some of them with high temporal distribution, such as radiometers, ground-based GPS (Global Positioning System) receivers and humidity sounding satellites. Each device has different advantages over the others. While radiosondes present relative humidity values with good vertical resolution, the radiometer and GPS receivers present IWV with good temporal resolution, and the humidity satellite sounding presents a good spatial coverage. Several comparison and intercomparison experiments of these devices have been carried out in the last years to characterize and to improve the accuracy of the atmospheric water vapor measurements. Radiosondes have been intercompared in several experiments and very important results to improve this technique have been obtained. Turner et al. 2003, Miller et al. 1999, Guichard et al. 2000, Miloshevich et al. 2001 and Wang et al. 2002 suggested the usage of an altitude-independent scale factor and corrections in the humidity measurement from the Vaisala RS80H radiosonde. As the RS80 is the most commonly used radiosonde nowadays, its performance was evaluated in operational usage comparing it with a more sophisticated humidity sensor (Paukkunen et al. 2001; Wang et al. 2001; Fujiwara et al. 2003). Several papers have shown GPS receiver performance in the quantification of atmospheric water vapor by comparing theirs results with those obtained from radiosondes and radiometers (Bevis et al. 1992; Duan et

al. 1996; Ware et al. 1997; Rocken et al. 1997; Emardson et al. 2000; Tsuda et al. 1998; Reigber et al. 2002; Marel 2001 and others). Radiosondes and GPS receivers were used in the validation of the new humidity measurement techniques, like solar radiometer (Ingold et al. 2000) and humidity sounding satellite (Wolfe and Gutman 2000) and were also used in experiments with intensive water vapor observation periods (Revercomb et al. 2003) to characterize and to improve the accuracy of the water vapor measurements.

The Amazonian region is characterized by large space-time variability in the humidity fields due to the intense convective process, which is frequent in this region, associated with the great humidity potential generated by high temperatures. This region is one of the most humid on the planet, where the IWV average is to the order of 50 kg m^{-2} (Sapucci et al. 2004). Nowadays, the impact of land use change on the climatological, ecological, biogeochemical and hydrological functioning of Amazonia and the interactions between Amazonia and the Earth's system are being investigated. Some researchers suspect that the increasing clearing of forest for agricultural activity will affect the hydrologic cycle (IWV in particular) and consequently the rainfall regime in several areas, making severe modifications to the global climate (Nobre et al. 1991; Manzi and Planton 1996). In this context, accessing the error associated with atmospheric humidity measurement and the validation of IWV quantification from indirect techniques, which can generate high spatial (satellite-based) and temporal (GPS receiver and radiometer) resolution, are very important in these regions.

An experiment with intensive collection of physical and chemical information from the atmosphere was accomplished in 2002, during the transition from the dry to wet season. This experiment is denominated RACCI/DRY-TO-WET (Radiation, Cloud, and Climate Interactions in Amazonia during the DRY-TO-WET Transition Season) (Silva Dias et al. 2002) and was carried out in several cities in the State of Rondônia, Brazil, where the clearing of forest for

agriculture and cattle raising is quite advanced. The main aim of RACCI is to understand the physical processes that control the transition season in Southwestern Amazonia and the regional effects of aerosols generated from biomass burning, which is quite common practice in this area at the end of the dry season. The interaction between these aerosols, the water vapor and liquid water is an important subject regarding the RACCI experiment. Consequently, IWV with high resolution contribute with the understanding of physics process involved in anthropogenic changes and the climate. IWV quantification by radiosondes, GPS receiver, radiometer and humidity sounding satellite was used to investigate the interaction between aerosols from biomass burning and physics process involved in the atmospheric water vapor cycle.

The goal of this study is to characterize the quality of IWV measurements from radiosondes, GPS receiver, solar radiometer and sounding satellite in the Amazonia region. The details of the instruments and collected data are described in section 2. In section 3 data processing from different techniques for water vapor atmospheric quantification is presented. The results obtained from the comparison of IWV from radiosondes, radiometer, humidity satellite sounding and the GPS receiver are presented in Section 4. In Section 5 the main results are summarized and conclusions are presented.

2. Instruments used and collected data for IWV quantification in the RACCI experiment

The RACCI experiment was composed of several sites with intensive collection of atmospheric information located in the Rondônia State into the Amazonian Region. The sites involved in the IWV experiment are called Abracos - Faz. N. Senhora, Guajará Mirim and Porto Velho, hereafter denominated the ABRA, GJMI and PTVE stations, respectively. Figure 1 shows the geographic localization of the RACCI experiment stations. The period of the experiment was

from 12 September to 3 November 2002. The instruments used in the IWV comparison experiment were:

Radiosonde: All radiosondes used were Vaisala, model RS80-15G. The launch times were 00 UTC, 12 UTC and 18 UTC in the ABRA station and 00 UTC and 12 UTC in the GJMI and PTVE stations. In the first and last 15 days of the campaign launching was intensified, with extra launches at 06 UTC, 15 UTC and 21 UTC in the ABRA station and 06 UTC and 18 UTC in the GJMI and PTVE stations. A total of 214 radiosondes were released in ABRA, 143 in GJMI and 110 in PTVE during the RACCI experiment.

Solar radiometer: In the ABRA station there is a CIMEL CE-318 Sun-Sky photometer operating since 1999 in the worldwide AERONET scope. The analysis of solar transmission measurements near the absorption band at 940 nanometers provides IWV several times between sunrise and sunset (Holben et al. 1998).

Humidity satellite sounding: The humidity from satellite sounding used here was obtained from AQUA satellite. The IWV retrieved from the AQUA satellite were obtained by the Humidity Sounder for Brazil (HSB) sensor (Lambrigtsen and Calheiros 2003).

GPS receiver: GPS data used to derive the IWV value during the RACCI experiment was collected using one ASHTECH receiver, ZXII model installed in the ABRA station (Marine C antenna), and two TOPCON brand, LEGACY-H model in the GJMI and PTVE stations (Legant E antenna). In the ABRA station the GPS antenna was installed in a metal base and in the GJMI station a metal stem, fixed on a building, was used. In the PTVE station it was installed in a tripod on the control tower at Porto Velho airport.

The data collect period for each measurement type in each site was not equal due to operational constraints related to the installation and uninstalling process for the devices

involved. Table 1 summarizes the collection period for each technique together with the geographic localization of the RACCI stations.

3. Data processing

The IWV from radiosondes were obtained applying the following expression

$$IWV = \int_{h_0}^{h} \rho_w dh \,. \tag{1}$$

with $\rho_w(z)$ the water vapor density at height z from h_0 to the top of the atmosphere h. The ρ_w was calculated using radiosonde dew point temperature and pressure measured along the atmospheric vertical column. The minimum height of the vertical column considered in this process was 8 km. A total of 14, 6 and 8 radiosondes in the ABRA, GJMI and PTVE stations, respectively, were discarded from the analysis because they did not reach this height or presented some other type of problems during launching.

Solar transmission measurements from the CIMEL instrument (AERONET) are typically performed every 15 minutes between sunrise and sunset, at selected wavelengths centered between 340 and 1020 nm. Holben et al. (1998) have discussed the operation and philosophy of the monitoring system, as well as the accuracy of the measuring radiometers. The IWV value is obtained from the CIMEL output voltage $V(\lambda)$ at wavelength λ applying following expression (Schmid et al. 2001):

$$IWV = \frac{1}{m}\left\{\frac{1}{a}\left[\ln\frac{V_0(\lambda)d^{-2}}{V(\lambda)} - m\left[\tau_R(\lambda)+\tau_a(\lambda)+\tau_3(\lambda)\right]\right]\right\}^{\frac{1}{b}}, \tag{2}$$

where m is the relative optical air mass, a function of the solar zenith angle, $V_0(\lambda)$ is the instrument calibration constant, d is the Earth-Sun distance, τ_R, τ_3 and τ_a are Raleigh scattering by air molecules, absorption owing to O_3 and attenuation caused by aerosol particles, respectively. The a and b are constants, whose were obtained using and LOWTRAN 7 radiative transfer model (Schmid et al. 2001). Such a procedure is meaningfully dependent on the representation of water vapor absorption that is adopted to provide the dataset of benchmark results from which a and b coefficients are derived. A first version of the AERONET was called level 1.5. However, previous studies have shown that the atmospheric transmittance at 940 nm (and hence estimates of water vapor content from solar transmission measurements at this band) can be substantially affected by changes in line parameters (Schmid et al. 2001), in the continuum model (Vogelmann et al. 1998) and even in the radiative transfer line-by-line model used for obtaining benchmark results (Plana-Fattori et al. 2004). The production of AERONET Level 2.0 results takes into account a recently updated algorithm for estimating the water vapor content. Such an update involves the application of a more reliable representation of the water vapor line and continuum absorption regimes near 940 nm, into a more reliable radiative transfer model (Dr. A. Smirnov, NASA/GSFC, personal communication, 2006).

The HSB was designed to detect radiances in the bands of 150 and 183 GHz with smaller susceptibility to radiofrequency than the AMSU-B sensor (Rosenkranz 2001). The HSB is composed of three channels around the absorption band of the water vapor (183.31 GHz ± 1, ± 3 and ± 7 GHz) and another one in the atmosphere window around 150 GHz. The HSB horizontal resolution is about 14 km in the nadir direction. IWV were retrieved only when the cloud cover was lower than 30%. Considering this constraint, the number of computed IWV was only 24, considering all stations (5 in ABRA, 11 in GJMI and 8 in PTVE). The IWV from the HSB sensor

were retrieved employing a method based on a lineal regression of the HSB channels (Lima and Machado 2006), in which the IWV in the layer *n* is express by:

$$IWV(n) = a(n) + \sum_{i=1}^{N} b_i(n) T_b(\nu_i), \quad (3)$$

where N is the number of HSB channel combinations used, $a(n)$ and $b_i(n)$ are regression coefficients and $Tb(\nu_i)$ is the brightness temperature measurement at ν_i frequency. The coefficients for this regression were obtained using the radiosondes launched in the RACCI experiment and RTTOV-7 radiative transfer model to simulate the brightness temperatures of the HSB channels (Lima and Machado 2006).

The zenithal tropospheric delay (Z_{TD}) were obtained by processing the GPS data using GOA-II software (Gregorius 1996) using the precise point positioning pos-processed method. This technique uses the absolute method (Duan et al. 1996) to retrieve IWV values, which does not require a reference IWV observation from another instrument. The zenithal wet delay (Z_{WD}) was obtained from Z_{TD} after removing the zenithal hydrostatic delay using an appropriated model (Davis et al. 1985), which requires the atmospheric pressure measurements. The Z_{WD} were converted into IWV by using the tropospheric mean temperature (Tm) together with the relationship suggested by Bevis et al. (1992):

$$IWV = Z_{WD} \frac{10^6}{R_w \left[k_2^{'} + \frac{k_3}{Tm} \right]}, \quad (4)$$

where R_w = (461.5181) $Jkg^{-1}K^{-1}$ is the specific gas constant for water vapor and $k_2^{'}$ and k_3 are atmospheric refractivity constants (Bevis et al. 1994).The Tm were obtained from temperature

(*Ts*) and pressure (*Ps*) measured at surface and applying a *Tm* model for the Amazonian Regions (Sapucci et al. 2006), which presents an RMS (Root Mean Square) values to the order of 1.8 K.

4. Results and discussion

As the radiosondes accomplish the humidity measurements in a direct way, the IWV from RS80 were used to analyze the results obtained from AERONET, the HSB sensor and GPS receivers. The results were presented using scatterplots (Figs 2, 3, 4 and 5) and the statistical information is given in tabular form in Table 2.

AERONET solar radiometer comparison with RS80 radiosondes. Figure 2 presents the scattering diagram of 38 data pairs between IWV from AERONET 1.5 level and RS80 radiosonde. We clearly see an overestimation of the IWV derived by AERONET 1.5 level. The Standard Deviation (S.D.) (2.0 kg m^{-2}) is much smaller than the bias (+6.5 kg m^{-2}), revealing that systematic error is present in this comparison. In addition, the correlation coefficient (*r*) between these techniques is large (*r* of 0.93) and the slope (1.03) indicates that AERONET and RS80 present similar sensitivity to IWV, although the interception value is also considerably large (+5.2 kg m^{-2}). Figure 2 also shows the discrepancies between the two techniques as a function of the RS80 IWV value. The adjusted line of discrepancies as a function of RS80 IWV (Fig. 2b) is parabolic in shape and shows that the largest disagreement between these techniques is in the interval between 37 and 45 kg m^{-2}, in which the dispersion is very large and the discrepancies in some cases were near 10 kg m^{-2}. If such a large bias was observed for the AERONET 1.5 level, for level 2.0 smaller discrepancies were observed. Figure 3 presents the scattering diagram of the IWV from AERONET 2.0 level as a function of RS80 IWV. Comparing Fig 3a to Fig. 2a it can

be seen that AERONET IWV from level 2.0 are drastically drier than level 1.5. Therefore, the large overestimate presented in the level 1.5 was removed in the level 2.0 (bias of -2.1 kg m^{-2}). Besides, the level 2.0 also presented important improvement in the precision of the IWV (S.D. 1.8 kg m^{-2}) and consequently, the RMS are significantly better in the level 2.0 (2.7 kg m^{-2}). The plot in Fig. 2b makes it evident that those discrepancies increase significantly when IWV becomes larger. The adjusted line of discrepancies is always negative showing that for IWV lower than 40 kg m^{-2} the tendency of the discrepancy nears the zero line, but decreases vertiginously otherwise. Version 2.0 corrected the wetter trend of version 1.5 by drying all and consequently, nearly all are drier than the radiosonde.

HSB sensor comparison with RS80 radiosondes. The results obtained in the comparison between IWV from the RS80 and HSB sensor are presented in Figure 4. Due to the constraint of nearly clear sky on producing HSB IWV values, very scarce during the RACCI experiment, only a small number of RS80-HSB coincident measurements (9 data pairs) were considered. HSB IWV is wetter than RS80 (bias of 1.9 kg m^{-2}) and the dispersion is very large (S.D. of 7.5 kg m^{-2}). The adjusted line of discrepancies (Fig. 4b) shows that this wetter tendency decreases when IWV become larger. The discrepancy tendency is initially positive and decreases crossing the zero line when IWV value is 41 kg m^{-2}. In addition, the slope value (0.28) reveals that the HSB and RS80 present different sensitivity to IWV and the interception value is quite large (+30.5 kg m^{-2}).

GPS receiver comparison with RS80 radiosonde. Figure 5 shows a scattering diagram and discrepancies from the GPS IWV as a function of the RS80 IWV ones. The scatter plots from Fig. 5 reveal that GPS technique presented a tendency to overestimate humidity in relation to the RS80 radiosonde. The observed bias were 3.2, 3.3 and 1.7 kg m^{-2} (or 6.3, 6.5 and 3.4 %), in the ABRA (Fig. 5a), GJMI (Fig. 5c) and PTVE (Fig. 5e) stations, respectively. Between GPS receiver and RS80 there was a substantial difference in the sensitivity to IWV values, as indicated

by the slope of the regression line. In the GJMI station, where the bias value is larger, the slope (0.95) value was closer to the unity than the one from PTVE (0.68) where the lowest bias was found. Another point worthy of attention in Fig. 5 is the large dispersion between the IWV from these techniques, mostly in the ABRA and GJMI stations, where the RMS in both stations were to the order of 4.0 kg m^{-2}. The IWV from PTVE presented the lowest dispersion (RMS value generated was 2.9 kg m^{-2}), but the correlation coefficient (r of 0.79) value reveals that the correlation between IWV from RS80 radiosondes in this station is worse than those from the ABRA and GJMI stations (r of 0.86 and 0.90, respectively). The adjust line of discrepancies in the ABRA and GJMI stations has a parabolic shape showing that the tendency is larger when the IWV is within the interval of 37 - 52 kg m^{-2}. This shape is similar to that generated in the comparison between IWV from AERONET and RS80 (Figs. 2b and 3b). In the PTVE station the adjust line of discrepancies has a rectilinear shape and shows that the discrepancy tendency is initially positive and decreases crossing the zero line and turning negative at the end, though the dispersion is larger along this adjust line. Probably, this difference in the adjust line shape is due to the difference in the range of IWV, because in the PTVE station they were above 42 kg m^{-2}, while in the other GPS stations 30 kg m^{-2} were obtained.

a. Analysis of the results

Table 2 summarizes the results of the various techniques used for measuring IWV, presenting statistical measurements and coefficients generated in the comparisons of all the possible combinations with RS80. In this analysis, the comparison between HSB and AERONET is not considered because there are only 3 data pairs available. An analysis of the numbers presented in this table shows the following:

→ The RS80 presents a tendency to underestimate the IWV when other techniques are considered as a reference (with the exception of the AERONET 2.0 level). This result is similar to ones obtained by other works, which reported that RS80 appears to have a dry bias (Turner et al. 2003; Revercomb et al. 2003; Sapucci et al. 2005);

→ The difference between IWV from AERONET 1.5 and 2.0 levels is around 18.5 % and is larger than expected. Schmid et al. (2001) reported that the IWV generated by the methodology applied in the 2.0 level is 13 % lower than in comparison with the AERONET 1.5 level;

→ It can be observed that IWV quantification from GPS tends to generate smaller values than those obtained from AERONET 1.5 level (bias of -2.33 kg m^{-2} or 4.5 %) and the correlation coefficient (*r*) between these techniques is the largest (*r* of 0.97). Previous intercomparison experiment showed that the AERONET IWV is about 6.8 % wetter than MWR (Microwave Radiometer) (Schmid et al. 2001). Emardson et al. (2000) using GPS data processing similar to the one used here, taking into account 141,864 pairs of data showed that GPS IWV are only 2.5 % wetter than MWR IWV values. These results suggest that GPS IWV is 4.3 % drier than CIMEL IWV values, which is a result near to the one generated in this comparison (4.5 %). However, when GPS IWV is compared to AERONET 2.0 level this tendency is very large and opposite (bias of -5.9 kg m^{-2}). In both AERONET levels the SD between these techniques was low;

→ The comparison between GPS and HSB sensor shows that HSB IWV is slightly wetter than GPS (bias of +1.0 kg m^{-2}, the lowest, or 2%), however, the dispersion is very large (S.D. of 4.15 kg m^{-2} or 8.1 %). The slope (0.68) reveal that HSB and GPS receiver present different sensitivity to IWV and the interception value is quite large (+14.168 kg m^{-2});

→ The tendency to overestimate humidity presented by the GPS technique, with relation to the RS80 radiosonde, is similar to results obtained in previous works, but at a lower magnitude. Emardson et al. (2000) using 1726 radiosondes showed that IWV from GPS data were 0.8 kg m^{-2} wetter than the ones from radiosonde data and Ingold et al. (2000) found a wetter bias of 1.76 kg m^{-2}. However, all these studies were not held over wetter tropical regions like the Amazon region.

On the contrary, the other comparisons between GPS and RS80 involved different devices in the three RACCI stations, for a total of 385 data pairs. These characteristics allow further investigation of the behavior of the discrepancies generated in this comparison. In the following section, a detailed tendency and dispersion analysis of the results is described.

b. Tendency and dispersion analysis of the GPS and RS80 comparison

Ionosphere-induced error can be one of the possible reasons for the bias that GPS IWV presented in comparison with RS80, which has been wetter than other intercomparison experiments. The free electrons in the ionosphere affect the propagation of the GPS signal (Leick 1995) generating error, such that is inversely proportional to the square of the carrier frequency and proportional to the total electron content (TEC) along the path between the satellite and receiver. The TEC is mainly a function of incident solar radiation flux that can vary by a wide range of phenomenon, such as: sunspot cycle, the rotation of the sun, the Earth's magnetic field, season and localization (Spilker 1994). Seeber (1993) describes this relation as a power series of $1/f$ (f is carrier frequency) where the higher-order terms are frequently ignored. The negligence of these terms in the GPS processing can result in residual errors related to the Z_{TD} during high solar activity (Brunner and Gu 1991), as in the Amazonian region during the RACCI experiment.

The most important factors influencing the ionospheric activity during the RACCI experiment were its location and the sunspot cycle (periodicity of approximately 11 years). The RACCI GPS stations were localized near the geomagnetic equator, in which the incident solar energy is larger than other regions, and the data collection was carried out during a period of high sunspot count, in which the terrestrial atmosphere ionization is intensified (Kunches 2001). The effects of sunspot counts on the GPS signal can be observed in the temporal series of the Earth's mean TEC (Figure 6) (Available at: http://www.aiub.unibe.ch/ionosphere.html>). The RACCI experiment was held close to the maximum period of sunspot cycle when the mean TEC values were sufficiently high (TEC of 40 10^{16}el m^{-2}), being four times larger than the minimum period in this cycle.

As the error in the GPS signal generated by ionosphere depend of the carried frequency, the TEC can be obtained applying a linear combination of P code from two carried frequencies: L1 at 1.57542 GHz and L2 at 1.22760 GHz (see Hofmann-Wellenhof et al. (2001) for more details). Figure 7 shows the line-of-sight TEC average as a function of local hours and the statistics generated in the different RACCI stations in order to show the correlation between the ionosphere's direct influence on the GPS signal and bias from the comparison between the GPS and RS80. The statistical information is shown in this figure as a function of the synoptic launching time of radiosondes because they are most used for operational purposes. The average TEC value varied substantially during the days of the RACCI experiment. Similar to results reported by Batista et al. (1994) related to the ionosphere in the equatorial region, the TEC maximum pick was around 14 LT (local time) and the minimum one was around 06 LT. During the day the TEC increases induced by incident solar energy, and the night it is reduced because the free electrons tend to recombine with ions.

As is clearly seen in Fig. 7, the bias is larger when the ionospheric activity is larger. The bias at 12 UTC (+3.9, +4.1 and +2.4 kg m^{-2} in the ABRA, GJMI and PTVE stations, respectively) and at 18 UTC (+4.3, +4.1 and +3.3 kg m^{-2}, respectively) is almost twice as larger as the bias from the radiosondes launched at 00 UTC (+1.9, +2.7 and +1.2 kg m^{-2}, respectively) and at 06 UTC (+1.1, +2.3 and -0.2 kg m^{-2}, respectively). Note that the best agreement is found in the radiosondes launched at 06 UTC (02 LT) and worst one to considering radiosondes at 18 UTC (14 LT).

The other point that needs to be considered is the RS80´s tendency in generating drier IWV during daytime than during nighttime. Turner et al. (2003), using a microwave radiometer, suggested that daytime RS80 is typically 3%-4% drier than nighttime. Sapucci et al. (2005), in a WMO radiosonde intercomparison experiment in Brazil, reported drier diurnal behavior to the order of 5.9% (or 2.9 kg m^{-2}, if RACCI IWV mean of 50.6 kg m^{-2} was considered) when RS80 is compared against the Snow White humidity sensor.

The period of the day in which ionospheric activity is larger coincides with the period where the largest wet bias from RS80 is observed. The combination of these two factors is probably the main reason for the fact that the bias found in this experiment is larger than in previous work results. If one considers only the nighttime radiosondes (where the ionospheric activity is reduced and the drier bias of the RS80 is lower) the bias value is of the same order as the results reported by Emardson et al. (2000) and Ingold et al. (2000), even though we are working over a very wet tropical region.

Van Baelen et al. (2005) using data from GPS receiver, RS90 radiosondes and microwave radiometer collected during a 3-month campaign in Toulouse, France, in the same period of the RACCI experiment, reported results similar to the ones found here. The difference between IWV from radiosonde and GPS receiver was clearly much larger at daytime than at

nighttime. Although the authors have not mentioned the high ionospheric activity in this period, it likely contributed for such results. Additionally, these authors reported that GPS IWV estimates, when compared to radiosondes, present a tendency almost linear from a significant negative bias (-1.0 kg m^{-2}) in dry atmospheric conditions (less than 15 kg m^{-2}) to very larger positive bias (+3,0 kg m^{-2}) in atmospheric conditions with larger humidity content (larger than 35 kg m^{-2}). Such tendency is confirmed in the results presented in the RACCI experiment, in which a bias of the 4.3 kg m^{-2} was obtained with IWV average in the order of 50 kg m^{-2}.

Another result that must be discussed is the different magnitude of the bias generated in PTVE (1.71 kg m^{-2}) and the other RACCI GPS stations (around 3.2 kg m^{-2} in ABRA and GJMI). In ABRA, in contrast with the other RACCI stations, the number of radiosondes launched during the daytime period (106 radiosondes) was much larger than the ones launched during the nighttime periods (61 radiosondes). Consequently, the influence of the ionosphere modeling residuals and RS80 daytime drier bias in the final bias in this station was more significant than the others. In order to investigate this assumption, analysis was carried out where only the simultaneous IWV-GPS and IWV-RS80 value pairs in three RACCI GPS stations were considered. The number of data pairs resultant was 61. In this circumstance, the bias value in the ABRA station was reduced from +3.2 to +2.3 kg m^{-2}, while in the other stations the bias remained practically unchanged (the bias remained +3.2 and +1.5 kg m^{-2} in GJMI and PTVE, respectively) as expected. The most probable reason for the different bias between the GJMI and PTVE stations is due to the multipath effects (see Hofmann-Wellenhof et al. (2001) for a detailed description) in the GPS signal reception. As the receiver brand and models are the same, the problem may be associated with the local where the receivers were installed. As the GJMI GPS receiver was installed over a roof, only few centimeters above it, this condition may generate more multipath than the PTVE receiver, which was installed in an open area. In order to

investigate this possibility, a quality control algorithm was applied based on TEQC (Translation Edit Quality Check) software (Estey and Meertens 1999). Therefore, it was possible to obtain the mean of the multipath of the GPS observables for the different stations, which are shown for one day as an example in Figure 8 (22 October 2002). From this figure one can observe that in the GJMI station there was a period (00 at 05 UTC) where the multipath effect is more significant than in the other stations. This period coincides with that one where the ionospheric activity is reduced and the RS80 drier bias is smaller. Consequently, the bias value in the GJMI station was kept relatively high during that period, while in the other stations it was considerably reduced. If only the radiosondes launched at 06 UTC is considered, the bias value in the GJMI station was +2.3 kg m^{-2}, while in ABRA and PTVE they were +1.1 kg m^{-2} and -0.2 kg m^{-2} respectively.

The S. D. was similar for the three stations (about of 4.5 % or 2.3 kg m^{-2}) and relatively better than the ones found in the other experiments. Emardson et al. (2000), using 1,726 radiosondes launched in European region (IWV medium of 20 kg m^{-2}), found S.D. to the order of 7.5 % (1.5 kg m^{-2}). Fig. 6 shows that the S.D. is nearly constant for different radiosonde launching time (about 2.0 kg m^{-2}) for all stations even under high ionospheric activity. This result is important because the S.D. is associated with stochastic error, and such reduced values provide an indication that the applied methodology is appropriated. Of course, the bias values, which are associated with systematic errors from the signal's multipath, high order ionosphere effects, and other non-modeled effects, significantly affected the RMS generated between the GPS and RS80 radiosondes. In the absence of such bias the resultant RMS would be similar to S.D. values.

5. Summary and conclusions

IWV retrieved from different techniques were analyzed during the RACCI experiment carried out in Amazonian Region on September and October 2002. Three remote IWV quantification techniques were used: two ground-based (GPS receivers and an AERONET photometer) and one space-based (HSB sensor), whose results were compared with RS80 radiosondes which, unlike the other techniques, accomplish the measurements in a direct way.

In summary, the results generated in the different comparisons suggest that RS80 presents a tendency to underestimate the IWV when compared against the other indirect techniques. The presence of some residuals of correction for the RS80 dry bias described by Wang et al. (2002) can have influenced this result. When compared to the GPS IWV values, it was shown that the AERONET 1.5 level and HSB sensor overestimate the IWV by +2.3 kg m^{-2} (+4.5 %) and +1.0 kg m^{-2} (1.9 %) respectively, while AERONET 2.0 level and RS80 underestimate by -5.9 kg m^{-2} (11.5 %) and -2.9 kg m^{-2} (5.7 %), respectively. The HSB sensor presented the lowest bias (in comparison with GPS), but also the worst dispersion (in the comparison with RS80) (RMS of 7.7 kg m^{-2}).

The new version of the IWV from AERONET (level 2.0) was able to remove the systematic error present in the level 1.5, which overestimates the IWV when compared with RS80. However, the results presented here shown that this new version underestimate the humidity for IWV above 40 kg m^{-2}. In this circumstance the AERONET level 2.0 generated IWV lower than RS80, which present suspect that it underestimates the atmospheric humidity.

The difference generated between IWV from the GPS receiver and the RS80 was high probably due the combination of the influence of Ionospheric effects (the RACCI experiment was carried out during a period of high ionospheric activity) in the GPS signal and drier daytime bias

of the RS80. If only the radiosondes launched during nighttime in the three stations are considered, the RMS value was of 2.7 kg m^{-2} (only 5.4 %) while for the ones launched during daytime the RMS value was 4.8 kg m^{-2} (8.6 %).

Acknowledgments

The authors wish to thank Maria Assunção F. Silva Dias (IAG-USP), coordinator of the RACCI experiment, for providing logistical support to the GPS data collection in this campaign; Santiago & Cintra Imp. and Exp. Ltda. for providing the Legacy receivers used in the experiment; coordinator of the SMOCC experiment and Fundação Universidade Federal de Rondônia (UNIR) and Destacamento de proteção ao Vôo de Porto Velho (DPVPV) for their assistance in the data collect; Brent Holben (NASA-GSFC) for its effort in establishing and maintaining Abracos_Hill AERONET site; Wagner Flauber Araujo Lima for HSB IWV values; Eder Paulo Vendrasco for radiosonde quality control; and Marcelo Tomio Matsuoka for important discussion about ionosphere activity in Amazonian region. This research was supported by FAPESP (Fundação de Amparo à Pesquisa do Estado de São Paulo) under Grants: Process N. 01/06908-7 and N. 01/12761-9.

REFERENCES

Batista, I.S., J.R. de Souza, M.A. Abdu and E.R. de Paula 1994: Total electron content at low latitude and its comparison with the IRI90. *Adv. Space Res.* **14** 12, Pages 87–90.

Bevis, M. G., S. Susinger, T. Herring, C. Rocken, R. A. Anthes and R. H. Ware, 1992: GPS meteorology: remote of atmospheric water vapor using the Global Positioning System. *Journal of Geophysical Research*, Vol. **97**, No. D14, Pages 15.787-15.801.

_____, S. Businger, S. Chiswell, T. Herring, R. A. Anthes, C. Rocken, R. H. Ware, 1994: GPS meteorology: mapping zenith wet delays into precipitable water. *J. Appl. Meteor*., **33**, 379-386.

Brunner F. K. and M. Gu, 1991: An improved model for the dual frequency inonospheric correction of GPS observations, *Manusc. Geod.*, **16**, 205-214.

Davis, J. L., T. A. Herring, I. Shapiro, A. E. Rogers and G. Elgened, 1985: Geodesy by interferometry: effects of atmospheric modeling errors on estimates of base line length. *Radio Sci.*, vol. **20**, 1593-1607.

Duan, J., M. Bevis, P. Fang, Y. Bock, S. Chiswell, S. Businger, C. Rocken, F. Solheim, T. Hove, R. Ware, S. Mcclusk, T. A. Herring and R. W. King, 1996: GPS meteorology: direct estimation of the absolute value of precipitable water, *Journal of Applied Meteorology*, vol. **35**, 830-838.

Emardson, T. R., J. M. Johansson and G. Elgered, 2000: The systematic behavior of water estimates using four years of GPS observation. *IEEE Transactions on Geoscience and Remote Sensing*. Vol. **38**, NO. 1, 324-329.

Estey, L. H. and C. M. Meertens, 1999: TEQC: The multi-purpose toolkit for GPS/GLONASS data. *Pub. by John Wiley & Sons*. Vol. **3**, No.1, 42-49.

Fujiwara , M., M. Shiotani, F. Hasebe, H. Vömel, S. J. Oltmans, P. W. Ruppert, T. Horinouchi, and T. Tsuda, 2003: Performance of the Meteolabor “Snow White” chilled-mirror

hygrometer in the tropical troposphere: Comparisons with the Vaisala RS80 A/H-Humicap sensors. *J. Atmos. Oceanic Technol*., **20**, 1534-1542.

Gregorius, T. 1996: How it works... GIPSY OASIS II, *Departament of Geomatics University of Newcastle upon Tyne*.

Guichard, F., D. Parsons and E. Miller, 2000: Thermo-dynamic and radiative impact of the correction of sounding humidity bias in the Tropics. *J. Climate*, **13**, 3615-3624.

Hofmann-Wellenhof, B., H. Lichtenegger and J. Collins, 2001: Global Positioning System Theory and Practice. 5.ed. New York: Springer-Verlag. 382p.

Holben, B. N., T. F.Eck, I. Slutsker, D. Tanre, J. P. Buis, A. Setzer, E. Vermote, J. A. Reagan, Y. J. Kaufman, T. Nakajima, F. Lavenu, I. Jankowiak and A. Smirnov. 1998: AERONET—A federated instrument network and data archive for aerosol characterization. *Remote Sens. Environ.* **66**, 1-66.

Ingold, T., B. Schmid, C. Mätzler, P. Demoulin and N. Kämpfer, 2000: Modeled and empirical approaches for retrieving columnar water vapor from solar transmittance measurements in the 0.72, 0.82 and 0.94 absorption bands. *Journal of geophysical research*, **105, NO. D19**, 24327-24343.

Kunches, J. M. 2001: In the Teeth of Cycle 23. Space Environment Center, NOAA. In: *IONGPS, International Technical Meeting* of Institute of Navigation, n. 14, 2001, Salk Lake City-Utah.

Kuo, Y. H., X. Zuo, and Y. R. Guo, 1996: Variational assimilation of precipitable water using nonhydrostatic mesoscale adjoins model. Part I: Moisture retrieval and sensitivity experiments. *Mon. Wea. Rev.*, **124**, 122-147.

Lambrigtsen, B. H. and R. V. Calheiros, 2003: The humidity sounder for Brazil – an international partnership. *IEEE Trans. Geosc. Remote Sensing*, **41**, pp 352-361.

Leick, A. 1995: GPS satellite surveying. 2. ed. New York: John Wiley & Sons, 560p.

Lima, W. F. A. and L. A. T. Machado, 2006: Análise do sensor HSB na estimativa do conteúdo integrado de vapor d'água: um estudo aplicado ao RACCI/LBA. "Analysis of integrated water vapor estimate from HSB sensor: a study applied to RACCI/LBA (In Portuguese)". *Brazilian Journal of Meteorology*. In press.

Manzi, A. and S. A. Planton, 1996: A simulation of Amazonian deforestation using a GCM calibrated with ABRACOS and ARME data. In: Gash, J. H. C., Nobre, C. A.; Roberts, J. M.; Victoria, R. L. eds. Amazonian Deforestation and Climate. Chichester: John Wiley, p. 505 - 529.

Marel, H., 2001: Exploitation of ground based GPS for numerical weather prediction and climate applications in Europe. *Delf University of Technology, Department of Geodesy*, Thijsseweg 11, 2629 J.A Delf, The Netherlands.

Miller, E. R., J. Wang, and H. L. Cole, 1999: Correction for dry bias in Vaisala radiosonde RH data. *Proc. Ninth Atmospheric Radiation Measurement (ARM) Science Team Meeting*, San Antonio, TX, U. S. Department. of Energy [Available online at http://www.arm.gov/ docs/documents/technical/ conf_9903/miller-er-99.pdf].

Miloshevich, L. M., H. Vömel, A. Paukkunen, A. J. Heymsfield, and S. J. Oltmans, 2001: Characterization and correction of relative humidity measurements from Vaisala RS80-A radiosondes at cold temperatures. *J. Atmos. Oceanic Technol*. **18**, 135-156.

Nobre, C. A., Sellers, P. J. and J. Shukla, 1991: Amazonian deforestation and regional climate change. *Journal of Climate*, v**.4**, p.957-988.

Paukkunen, A., V. Antikainem and H. Jauhiainen, 2001: Accuracy and performance of the new Vaisala RS90 radiosonde in operational use. *11th Symposium on Meteorological Observations and Instrumentation*. Albuquerque, New Mexico, USA.

Plana-Fattori, A., P. Dubuisson, B. A. Fomin, and M. P. Correa, 2004: Estimating the atmospheric water vapor content from multi-filter rotating shadow-band radiometry at Sao Paulo, Brazil. *Atmospheric Research*, **71,** 171-192.

Reigber, C., G. Gendt, G. Dick and M. Tomassini, 2002: Near real-time water vapor monitoring for weather forecast. *GPS world*. January, 18-27.

Revercomb, H. E., D. D. Turner, D. C. Tobin, R. O. Knuteson, W. F. Feltz, J. Barnand, J. Bösenberg, S. Clough, D. Cook, R. Ferrere, J. Goldsmith, S. Gutman, R. Halhore, B. Lesht, J. Liljegren, H. Linné, J. Michalsky, V. Morris, W. Porch, S. Richardson, B. Schimid, M. Splitt, T. Van Hove, E. Westwater, and D. Whiteman, 2003: The ARM program's water vapor intensive observation periods. Overview, initial accomplishments, and Future Challenges. *Bull. Am. Met. Soc*., **84**; 2, 217-236.

Rocken, C., T. Van Hove and R. H. Ware, 1997: Near real-time GPS sensing of atmospheric water vapor. *Geophy. Res Lett.*, **24**, 3221-3224.

Rosenkranz, P. W. 2001: Retrieval of temperature and moisture profiles from AMSU-A and AMSU-B measurements. IEEE Trans. *Geosci. and Remote Sensing*, **39**, 2429-2435, 2001.

Sapucci, L. F.; J. F. G. Monico, A. Plana-Fattori, L. A. T. Machado and W. F. A. Lima, 2004: GPS Performance in the Quantification of Integrated Water Vapor in Amazonian Regions. In: *IONGNSS, International Technical Meeting* of Institute of Navigation, n. 17, 2004, Long Beach – California.

Sapucci, L. F., L. A. T. Machado, R. B. Silveira, G. Fisch and J. F. G. Monico, 2005: Analysis of relative humidity sensors at WMO radiosonde intercomparison experiment in Brazil. *J. Atmos. Oceanic Technol.*, **22**, 6, 664-678.

Sapucci, L. F., L. A. T. Machado and J. F. G. Monico. 2006: Brazilian model for tropospheric mean temperature from surface measurements. *"In preparation". GPS Solution*.

Schmid, B., J. Michalsky, D. W. Slater, J. C. Barnard, R. N. Halthore, J. C. Liljegren, B. N. Holben, T. F. Eck, J. M. Livingston P. B. Russell, T. Ingold and I. Slutsker, 2001: Comparison of columnar water-vapor measurements from solar transmittance methods. *Applied Optics*, **40**, N. 12, 1986-1896.

Seeber, G., 1993: Satellite Geodesy: Foundations, Methods and Applications. Berlin-New York: Walter de Gruyter, 531p.

Silva Dias, M. A. F., S. Rutledge, P. Kabat, P. L. Dias, C. A. Nobre, G. Fisch, A. J. Dolman, E. Zipser, M. Garstang, A. O. Manzi, J. Fuentes, H. R. Rocha, J. Marengo, A. Plana-Fattori, L. Sá, R. Alvalá, M. Andreae, P. Artaxo, R. Gielow and L. Gatti, 2002: Clouds and rain processes in a biosphere atmosphere interaction context in the Amazon Region. *Journal of Geophysical Research*, Estados Unidos, v. **107**, n. D20, p. 46.1-46.23.

Spilker JR, J. J., 1994: Tropospheric effects on GPS. In Parkinson, B. W. & Spilker Jr. J. J. Global Positioning System: Theory and Applications, Vol. 1, Chapter 13, pp. 517-546.

Tsuda, T., K. Heki, S. Miyazaki, K. Aonashi, K. Hirahara, H. Nakamura, M. Tobita, F. Kimata, T. Tabei, T. Matsushima, F. Kimura, M. Satomura, T. Kato, and I. Naito, 1998: GPS meteorology project of Japan - exploring frontiers of geodesy. *Research News Earth Planets Space*, **50**(10), i–v.

Turner, D. D., B. M. Lesht, S. A. Clough, J. C. Liljegren, H. E. Revercomb, and D. C. Tobin, 2003: Dry bias and variability in Vaisala RS80-H radiosondes: The ARM experience. *J. Atmos. Oceanic Technol.*, **20**, 117-132.

Van Baelen, J., J. P. Albagnag and A. Dabas, 2005: Comparison of near real time estimates of integrated water vapor derived with GPS, radiosondes and microwave radiometer. *J. Atmos. Oceanic Technol*. **22**, 201-210.

Vogelmann, A.M., V. Ramanathan, W.C. Conant and W.E. Hunter, 1998: Observational constraints on non-Lorentzian continuum effects in the near-infrared solar spectrum using ARM ARESE data. *Journal of Quantitative Spectroscopy and Radiative Transfer*, **60**(2), 231-246.

Wang, J., H. L. Cole, D. J. Carlson, E. R. Miller, and K. Beierle, A Paukkunen and T. K. Laine, 2002: Corrections of humidity measurements errors from the Vaisala RS80 radiosonde – Application to TOGA CARE data. *J. Atmos. Oceanic Technol*. **19**, 981-1002.

_____., _____, D. J. Carlson and A. Paukkunen, 2001: Performance of Vaisala RS80 Radiosonde on measuring upper-tropospheric humidity after corrections. *11th Synposium on Meteorological Observations and Instrumentation.* Albuquerque, New Mexico, USA.

Ware, R., C. Alber, C. Rocken and F. Solheim, 1997: Sensing integrated water vapor along GPS ray paths. *Geophys. Res. Lett.*, **24**, 417-420.

Wolfe, D. E. and S. I. Gutman, 2000: Developing an operational, surface-based, GPS, water vapor observing system for NOAA: network design and results. *J. Atmos. Oceanic Technol*. **17**, 426-440

Figure Captions

Figure 1 - Geographic localization of the RACCI experiment stations.

Figure 2 - Scattering diagrams of the AERONET IWV from level 1.5 (a) and discrepancies (b) as a function of the RS80 IWV in the ABRA station.

Figure 3 - Same as Fig. 2, but using AERONET IWV from level 2.0.

Figure 4 - Scattering diagrams of the HSB IWV as a function of the RS80 IWV in the ABRA, GJMI and PTVE stations.

Figure 5 - Scattering diagrams of the GPS IWV from RACCI GPS stations as a function of the RS80 IWV values.

Figure 6 – Time series of the Earth's mean TEC from 1 January 1995 to 6 February 2006 (Source: Center for Orbit Determination in Europe. Available in: http://www.aiub.unibe.ch/ionosphere.html>).

Figure 7 - The line-of-sight TEC average as a function of local time (LT) and statistical measurements of the comparison between the GPS and RS80 in function radiosonde launching synoptic time.

Figure 8 - Mean of multipath in the GPS signal in the three RACCI GPS stations (6 October 2002).

Tables

TABLE 1 Sites and periods of data collection under consideration in this study.

RACCI Station	Latitude	Longitude	Collect Period	Radiosonde launching	GPS receiver	HSB Sensor	AERONET radiometer
ABRA	10°45'S	62°21'W	Begin	Sep. 12th	Sep. 21st	Sep. 12th	Sep. 01st
			End	Nov. 03rd	Nov. 03rd	Nov. 03rd	Nov. 15th
PTVE	08°42'S	63°53'W	Begin	Sep. 20th	Sep. 18th	Sep. 12th	…
			End	Oct. 29th	Oct. 29th	Nov. 03rd	…
GJMI	10°45'S	65°18'W	Begin	Sep. 15th	Sep. 15th	Sep. 12th	…
			End	Oct. 28th	Oct. 28th	Nov. 03rd	…

TABLE 2. Statistical measurements and coefficient generated in the several comparisons between different IWV quantification techniques used in the RACCI experiment.

Comparison	Number of considered data pairs	Statistical measurement			Coefficient		
		Bias (kg m^{-2})	S. D. (kg m^{-2})	RMS (kg m^{-2})	Correlation	Slope	Intercept
AERONET (1.5) - RS80 ABRA	38	**+6.470**	2.045	6.785	0.928	**1.029**	+5.242
AERONET (2.0) - RS80 ABRA	33	-2.065	1.783	**2.729**	0.799	6.389	**0.928**
HSB - RS80 All station	9	+1.907	**7.471**	**7.711**	**0.559**	**0.287**	**30.457**
GPS - RS80 ABRA	167	+3.167	2.463	4.012	0.857	0.784	+12.826
GPS - RS80 GJMI	121	+3.279	2.354	4.037	0.902	0.948	+5.545
GPS - RS80 PTVE	97	+1.710	2.281	2.851	0.791	0.678	+17.597
AERONET (1.5) - GPS ABRA	298	+2.328	**1.640**	2.848	**0.966**	0.819	+6.328
AERONET (2.0) - GPS ABRA	295	-5.938	**1.679**	6.171	0.940	1.051	+3.944
HSB - GPS All station	24	**+1.006**	4.152	4.272	0.788	0.678	+14.168

Figures

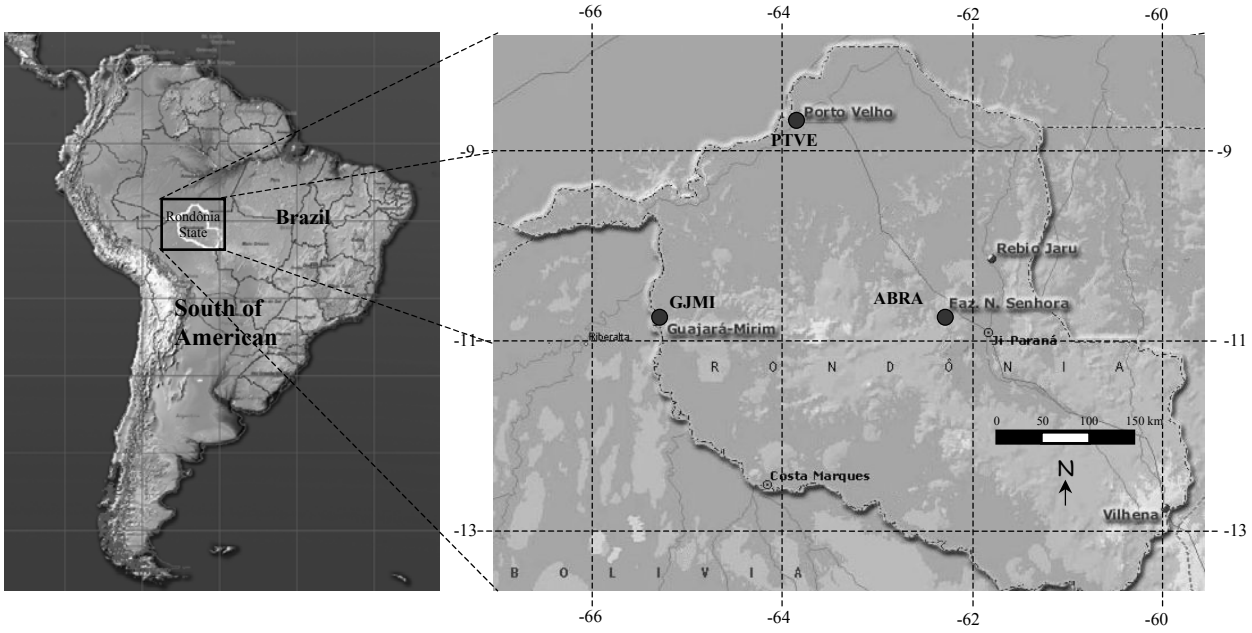

Figure 1

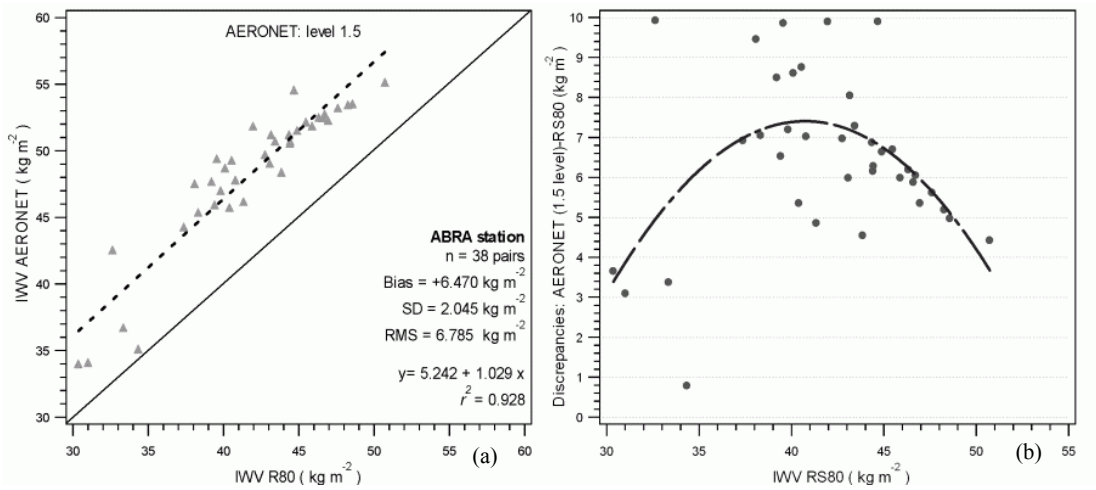

Figure 2

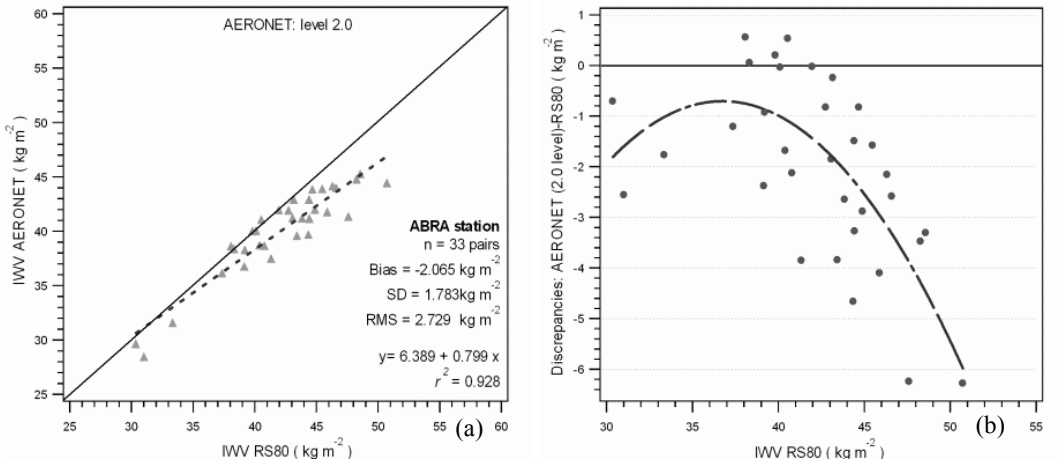

Figure 3

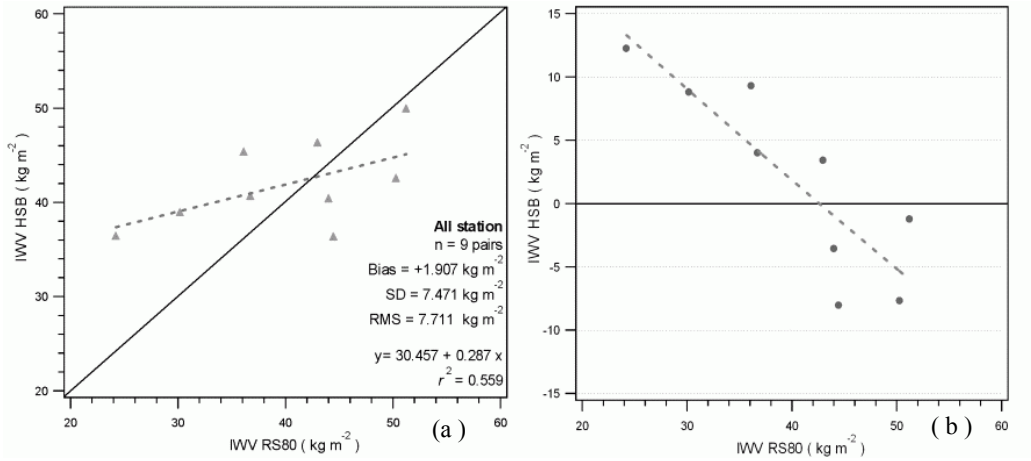

Figure 4

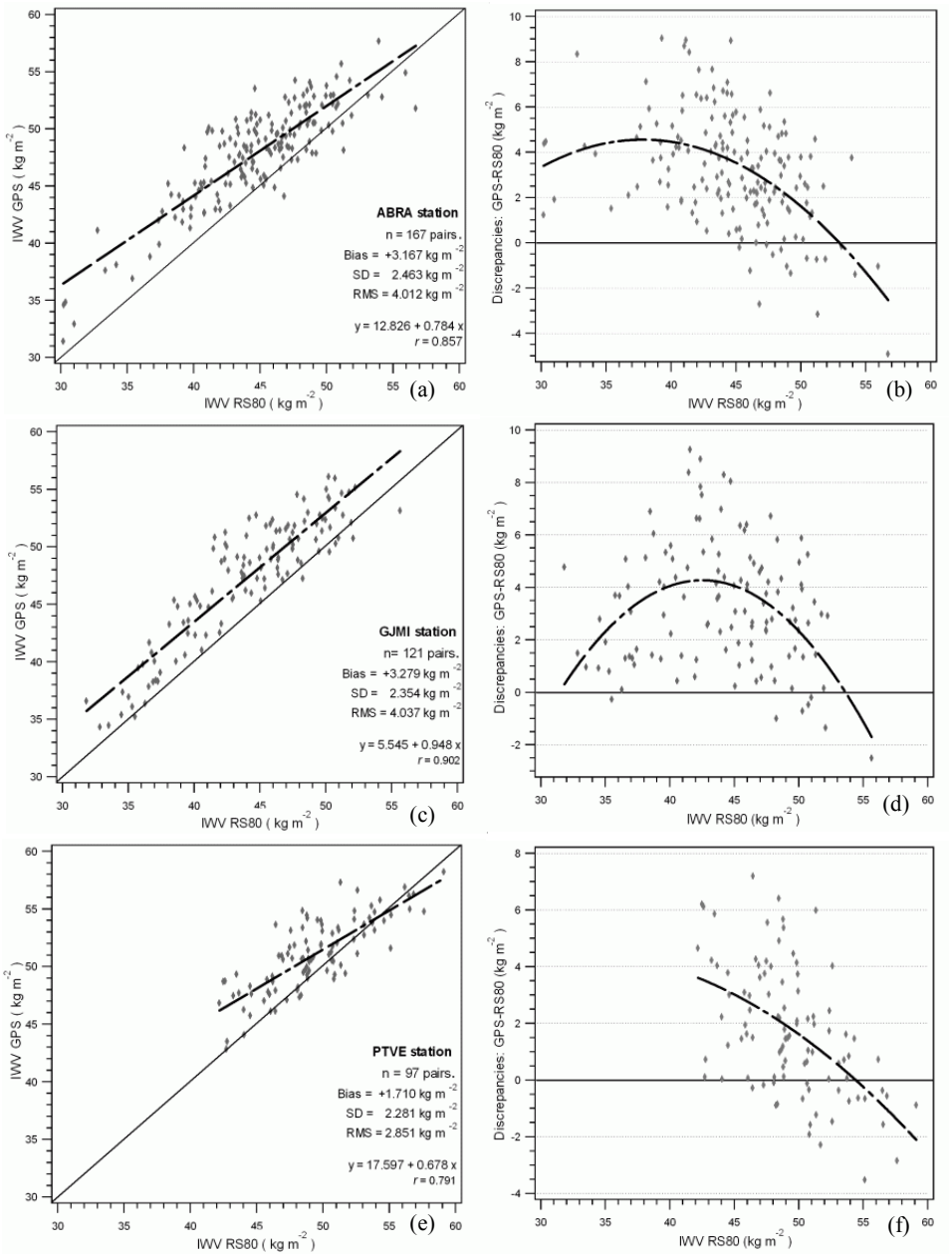
IWV GPS (kg m-2)
IWV RS80 (kg m-2)
ABRA station
n = 167 pairs.
Bias = +3.167 kg m-2
SD = 2.463 kg m-2
RMS = 4.012 kg m-2
y = 12.826 + 0.784 x
r = 0.857
(a)
Discrepancies: GPS-RS80 (kg m-2)
IWV RS80 (kg m-2)
(b)
GJMI station
n= 121 pairs.
Bias = +3.279 kg m-2
SD = 2.354 kg m-2
RMS = 4.037 kg m-2
y = 5.545 + 0.948 x
r = 0.902
(c)
(d)
PTVE station
n = 97 pairs.
Bias = +1.710 kg m-2
SD = 2.281 kg m-2
RMS = 2.851 kg m-2
y = 17.597 + 0.678 x
r = 0.791
(e)
(f)

Figure 5

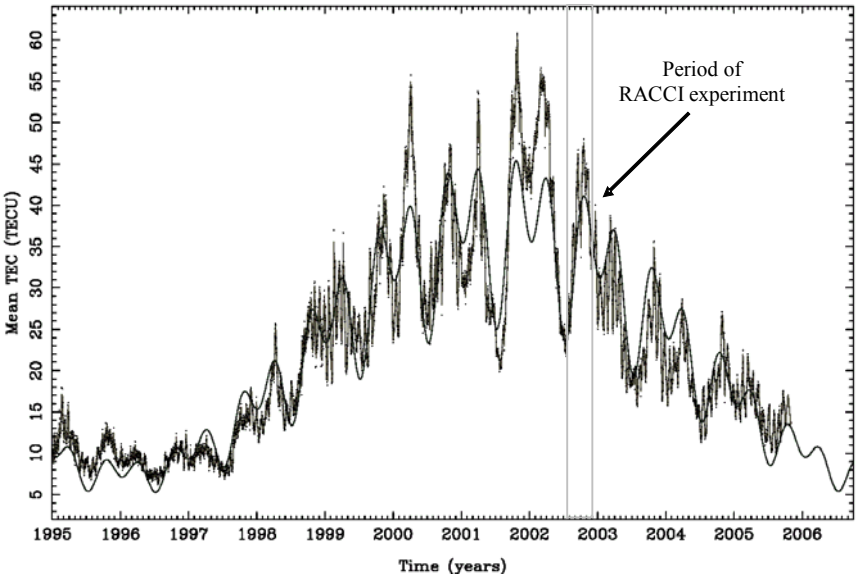
Period of
RACCI experiment
Mean TEC (TECU)
Time (years)
5
10
15
20
25
30
35
40
45
50
55
60
1995
1996
1997
1998
1999
2000
2001
2002
2003
2004
2005
2006

Figure 6

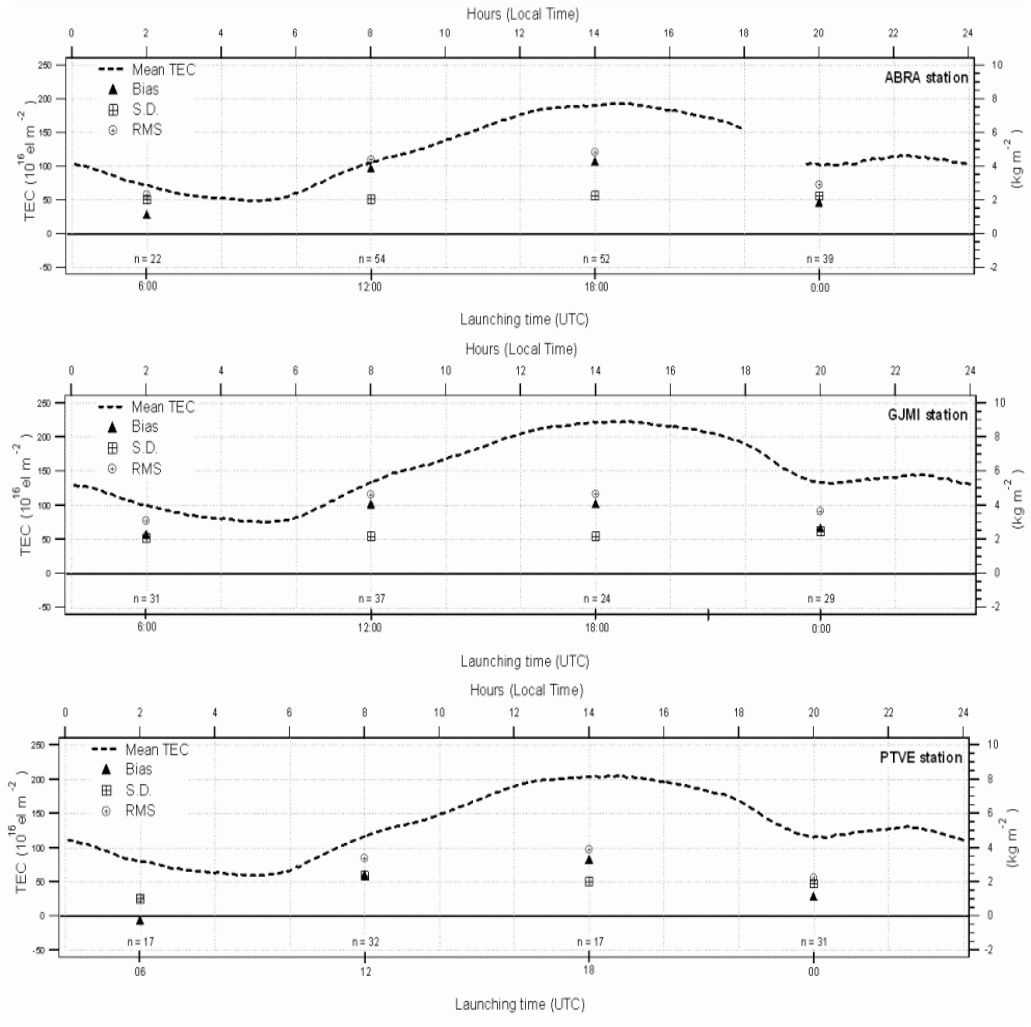

Figure 7

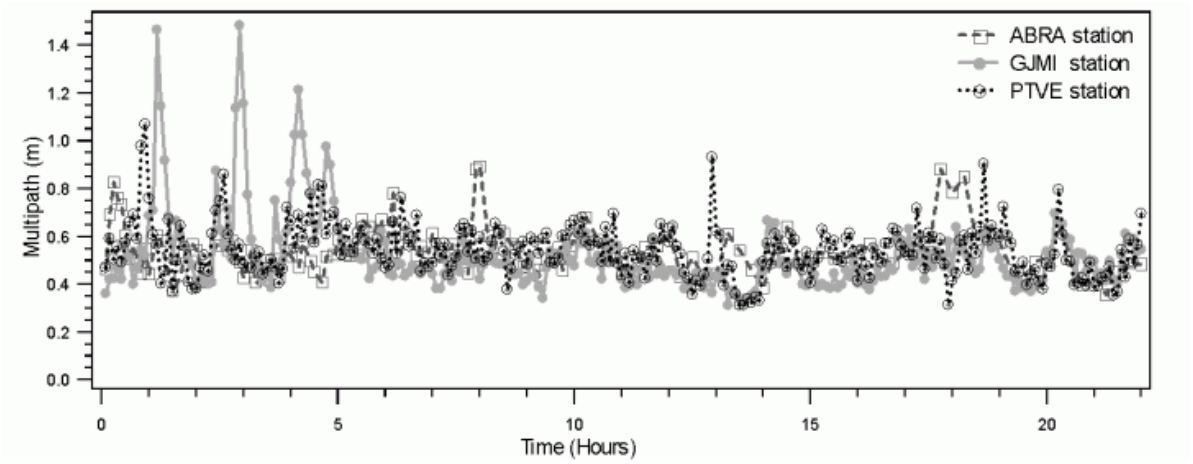

Figure 8